Mohd Sufian OTHMAN[1], Mohd Zaki NUAWI[1], Ramizi MOHAMED[2]
Universiti Kebangsaan Malaysia, Dept. of Mechanical & Material Eng. (1), Dept. of Electrical, Electronic & Systems Eng. (2)

doi:10.15199/48.2016.11.51

Experimental Comparison of Vibration and Acoustic Emission Signal Analysis Using Kurtosis-Based Methods for Induction Motor Bearing Condition Monitoring

Abstract. *Vibration and acoustic emission (AE) signal measurement are established tools in condition monitoring of bearings. This paper presents a comparison between two statistical methods, i.e. kurtosis, and another kurtosis based method called I-kaz using simultaneous signal of vibration and AE. The existence of harmonics fault frequencies in envelope spectrums also have been discussed. The results reveal that both signals are suitable for induction motor bearing fault detection.*

Streszczenie. *W artykule przedstawiono porównanie dwóch metod statystycznych, kurtozy oraz I-kaz używających do diagnostyki łożyskowania maszyn elektrycznych. Jako sygnały diagnostyczne wykorzystuje się pomiar wibracji i emisji akustycznej.(**Eksperymentalne porównanie drgań i analizy sygnałów emisji akustycznej do monitorowania stanu łożysk**).*

Keywords: bearing fault, kurtosis, I-kaz.
Słowa kluczowe: monitorowanie stanu łożyska, kurtoza, I-kaz.

1. Introduction

Bearing is one of important components in rotating machines that enable smooth acceleration and reduce friction. Ball and roller bearing are common type of bearing used in induction motors. Normally, an induction motor has two bearings supporting the rotor shaft; at the fan-end side, and at the drive-end side. The faulty bearing can cause major defects to motor if not fixed in a timely manner. The common failure observed in bearing elements are inner race fault and outer race fault.

Vibration analysis is the most widely used technique for fault detection of rotating machineries and components such as bearings and gears. As vibration can be represented by the displacement, velocity or acceleration, any sensor that measure any of these variables can be used. Piezoelectric accelerometer is the most popular detector used to measure vibration because of rugged, small and relatively inexpensive [1]. Therefore, this study focused on acceleration measurement using an accelerometer. Acoustic emission (AE) is the phenomena of transient elastic wave generation as a result of fast strain energy discharge from deformation or localised damage within or on material surface [2], [3]. Combination of vibration and AE measurement in bearing diagnostics has been done by Al-Ghamd and Mba [4], Eftekharnejad et al. [5], and Liu et al [6] using various methods.

Statistical analysis is one of the earliest approaches for bearing fault detection in time-domain. The calculation of crest factor, which is the ratio of peak value to the root mean square (RMS) value of signal data have been the simplest approach to detect bearing faults in time domain analysis [7]. However, this method had limited success in the detection of localized defects. Generally, most of parameters used in the time domain are derived from statistical moment of data. The first and second moments are well known, being the mean and the variance respectively. For N numbers of data set ($y_1, y_2, \ldots, y_n$), the mean, μ and the variance, σ can be calculated as:

$$\mu = \frac{1}{N}\sum_{n=1}^{N}\left(y_n\right) . \tag{1}$$

$$\sigma = \frac{1}{N}\sum_{n=1}^{N}\left(y_n - \mu\right)^2 . \tag{2}$$

The third and fourth moments, the skewness (*Sk*) and the kurtosis (*Kur*) respectively, defined as

$$Sk = \frac{\frac{1}{N}\sum_{n=1}^{N}\left(y_n - \mu\right)^3}{s^3} . \tag{3}$$

$$Kur = \frac{\frac{1}{N}\sum_{n=1}^{N}\left(y_n - \mu\right)^4}{s^4} . \tag{4}$$

where s, is the square root of the variance, or the standard deviation as stated in Eq. 5.

$$s = \sqrt{\sigma} . \tag{5}$$

The usage of kurtosis for bearing fault detection was first proposed by Dyer and Stewart in 1978 [8]. For a good condition bearing with normal or Gaussian distribution, the kurtosis value is close to 3. However, when the fault is well advanced, the kurtosis value was reported to come down to the same value as undamaged bearing which is 3. Therefore, to solve this issue they have suggested to measure kurtosis in selected frequency bands. Furthermore, kurtosis also have been applied in Spectral Kurtosis analysis [9], [10], or also known as kurtogram method [11], [12] for detection of bearing fault in frequency domain. Another great kurtosis-based method is the integrated kurtosis-based algorithm for z-filter technique (I-kaz) proposed by Nuawi et al [13]. This method provides an I-kaz coefficient and a three dimensional graph with low, high, and very high frequency range which are represented in x-axis, y-axis, and z-axis respectively. Detail of signal decomposition process is as follows:

- Low frequency range (L): 0 to 0.25 f_{max}
- High frequency range (H): 0.25 to 0.5 f_{max}
- Very high frequency range (V): 0.5 f_{max} to f_{max}

where f_{max} is the half value of the data sampling rate. I-kaz coefficient, Z^{∞} is derived from the kurtosis and standard deviation from all frequency ranges, as in Eq. 6.

$$Z^{\infty} = \frac{1}{N}\sqrt{Kur_L \cdot {s_L}^4 + Kur_H \cdot {s_H}^4 + Kur_V \cdot {s_V}^4} . \tag{6}$$

The I-kaz method have been successfully applied for condition monitoring of car engine bearing [14], engine block [15], suspension system [16], machine cutting tool [17]–[19], and charpy impact tester [20].

This paper presents a comparison of vibration and AE signal analysis using three fault detection techniques, i.e. (1) time-domain waveform analysis using kurtosis method and envelope spectrum analysis to locate fault frequencies, (2) I-kaz graphical and coefficient methods, and (3) comparative study of I-kaz coefficient against kurtosis.

2. Methodology

The proposed work flow chart for this research is shown in Fig. 1. The process was started with an experimental test rig setup followed by data acquisition with two types of sensors: (a) accelerometer for measuring vibration signal, and (b) AE transducer for acoustic emission signal. Data were collected and stored in the computer before analysis using MATLAB version 8.3 have been done.

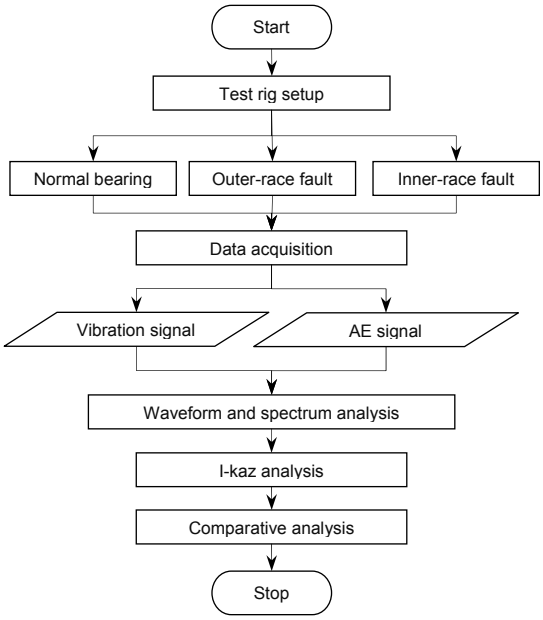

Fig. 1: Proposed research flowchart

The experimental tests were performed on a test rig consist of a low speed 4 pole induction motor with the rated speed of 1405 rpm (See Table 1). The motor was supplied by the 3 phase variable voltage transformer pre-set at 380V. Tacho generator was connected to the drive-end of motor to measure the rotation speed of the induction motor. A magnetic powder brake was coupled to the other end of tacho generator. This magnetic brake used to apply axial loads to the motor, controlled by the control unit. The details of test rig setup are shown in Fig. 2.

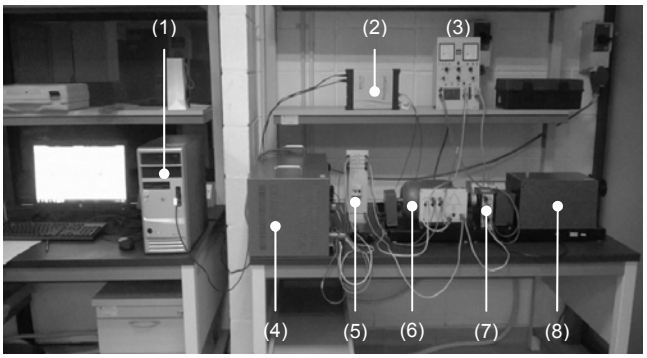

Fig. 2: Experimental setup: (1) computer, (2) oscilloscope, (3) control unit, (4) 3 phase variable voltage supply, (5) motor protection switch, (6) squirrel cage induction motor, (7) tacho generator, and (8) magnetic powder brake.

Table 1: Motor Specification (Nameplate)

Make	Leybold Didactic GmbH
Model Number	732 94
Rated Power	0.7 kW
Rated Speed	1405 min^{-1}
Frequency	50 Hz
Starting Current	2.0 A

Three bearing condition have been tested using the same motor which are normal bearing, bearing with inner race fault, and bearing with outer race fault. All faulty bearings have been artificially damaged by axial drilled of a 1mm hole through the raceways (see Fig. 3).

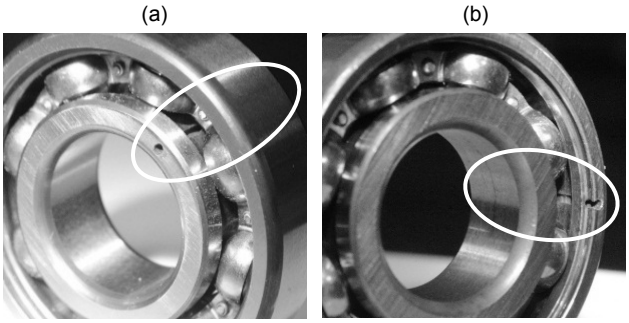

Fig. 3**:** Tested bearing with artificial localized defect at (a) inner race and (b) outer race.

The motor has been tested with different tork applied started with 0 Nm and increased 1 Nm until reach full load (3 Nm). The motor shaft speed were measured and recorded as tabulated in Table 2.

Table 2: Motor shaft speeds at different tork.

Tork	0 Nm	1 Nm	2 Nm	3 Nm
Speed	1450 rpm	1430 rpm	1420 rpm	1380 rpm

Tested bearing was placed on the drive-end of the motor. Detail information about the tested bearing is stated in Table 3. Vibration signal was measured using Endevco 751-100 piezoelectric accelerometer with sensitivity of 100mV/g and a DeCI SE1000H acoustic emission transducer with sensitivity of 100V/μm used to collect AE signal (Fig. 4).

Data were sampled at 99,968 Hz using PicoScope 6402A oscilloscope at one second time frame and stored in 32 files. Hence, the total acquired are 3,198,176 data. Collected data for both signals were in voltage (V). For the vibration signal, the data have been converted to acceleration (g/ms^{-2}) to represent vibration by dividing the voltage to sensor sensitivity value.

Table 3: Testing bearing information

Bearing Number	*FAG 6204ZR C3*
Bearing outer diameter	*47mm*
Bearing inner diameter	*20mm*
Bearing width	*14mm*
Ball diameter	*7.938mm*
Number of balls	*8*
Contact angle	*0°*

Table 4: Tested Bearing Fault Frequencies at Different Shaft Speeds in Hertz (Hz).

Frequency Name	1380 rpm	1450 rpm
Shaft frequency, f_S	23.0	24.2
Inner race fault (BPFI), f_{IR}	113.8	119.6
Outer race fault (BPFO), f_{OR}	70.2	73.8

Table 4 is presented the tested bearing fault frequencies in four different shaft speed. In this table, 1380 rpm is for full load and 1450 rpm is for no load. These fault frequencies were used in the envelope spectrum analysis in frequency-domain plots.

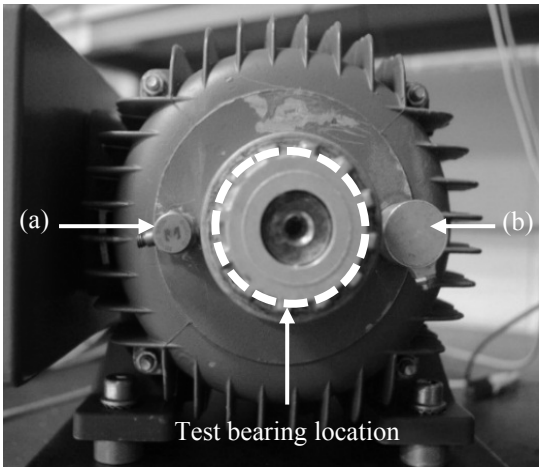

Fig. 4: Sensor location on motor casing: (a) Piezoelectric accelerometer, and (b) AE transducer.

3. Results and Discussion

Three analyses have been carried out; i.e. (a) waveform and spectrum comparison, (b) I-kaz analysis, and (c) comparative analysis. The results show in the following sub-section were taken from the first file out of 32 except for sub-section 3.3. which was a combination of all data.

3.1 Time Waveform & Envelope Spectrum Analysis

In the time waveform analysis, kurtosis value of acceleration and AE signal have been compared between normal and faulty bearing. The results were grouped and presented based on motor speeds and loads. On the other hand, fundamental and harmonic fault frequencies in envelope spectrum plots also have been observed and reported accordingly.

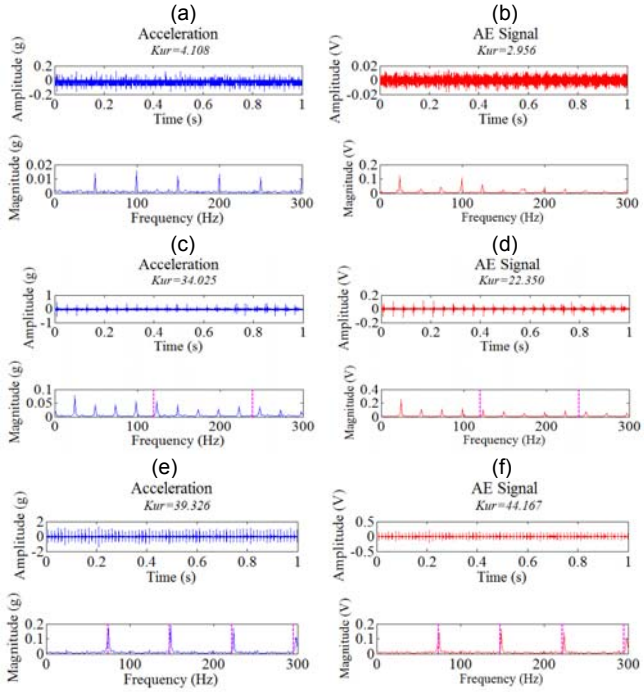

Fig. 5: Comparison of time waveform and envelope spectrum for acceleration and AE signal of the motor running at 1450 rpm (no load) with (a),(b) normal, (c),(d) inner race faulty, and (e),(f) outer race faulty bearing.

Time waveform and envelope spectrum of vibration and AE signal are shown in Fig. 5 and Fig. 6, represented no load and full load respectively. In all these figures, (a), (c), and (e) are plots for acceleration and (b), (d), and (f) are for the AE signal. In no load plots, the kurtosis of normal bearing is close to 3 for both acceleration and AE signal, proved that the data are normally distributed [Refer Fig. 5(a) and Fig. 5(b)]. Kurtosis values for faulty bearings are significantly higher than 3 as shown in Fig. 5(c) to Fig. 5(f).

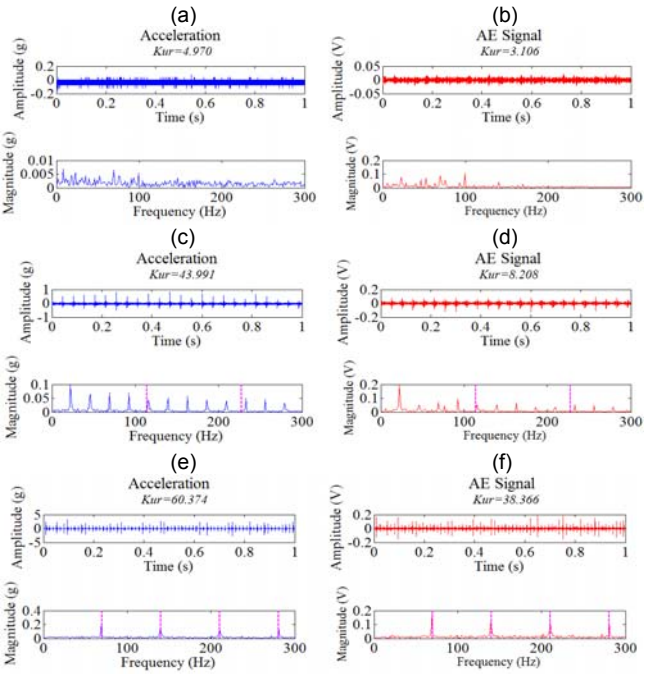

Fig. 6: Comparison of time waveform and envelope spectrum for acceleration and AE signal of the motor running at 1380 rpm (full load) with (a),(b) normal, (c),(d) inner race faulty, and (e),(f) outer race faulty bearing.

Same notification also observed in full load except for the kurtosis value of AE signal in the inner race faulty bearing which was considered small compared to acceleration signal on the left side [see Fig. 6(c) and Fig. 6(d)]. In both no load and full load envelope analysis, the outer race fault frequency and it repetitions are clearly observed for both acceleration and AE signal [See Fig. 5 (e),(f) and Fig. 6(e),(f)]. However, for the inner race fault, the repetition frequencies are not discovered, although the fault frequency appeared perfectly [See Fig. 5(c),(d) and Fig. 6(c),(d)].

3.2 I-kaz Analysis

The shape and the scattering of graphical I-kaz plots for acceleration and AE signal were observed and compared between normal and faulty bearing to check for any discrepancy. In addition, the I-kaz coefficient (Z^{∞}) for each plots also have been analysed. Axis ranges for all plots in each figure have been standardised for easy and equal comparison.

Results for I-kaz analysis are displayed in Fig. 7 for no load and Fig. 8 for full load. It is observed that all graphical I-kaz plots provided clear identification to verify bearing conditions accordingly. For normal bearing, both acceleration and AE signal data are concentrated at same slot for all low, high and very high frequency ranges with Z^{∞} for acceleration signal is quite similar for no load and full load plots whereas Z^{∞} for AE signal for no load is slightly smaller than full load plot. Different finding is observed for faulty bearings where Z^{∞} for acceleration data of inner race and outer race faults in full load were larger than in no load, but Z^{∞} for AE data in full load was smaller than in no load plots. However, when comparing separately in the same figure, the I-kaz coefficient values for acceleration and AE signal in both no load (Fig. 7) and full load (Fig. 8) shown

significant increment between normal and damaged bearings. For example, the Z^{∞} for acceleration signal of normal bearing is 4.286×10^{-9} as in Fig. 7(a), 3.77×10^{-8} for inner race fault as in Fig. 7(c), and 3.348×10^{-7} for outer race fault as in Fig. 7(e).

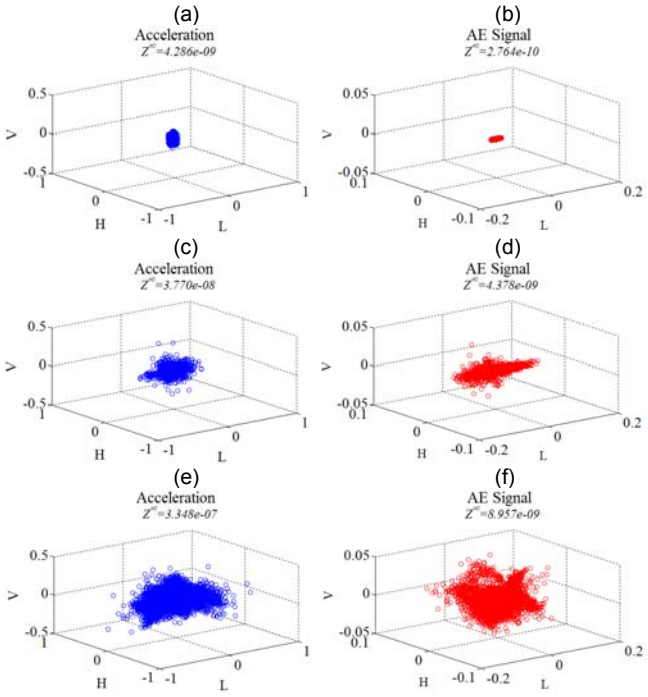

Fig. 7. Comparison of I-kaz graphic and coefficient for acceleration and AE signal of the motor running at 1450 rpm (no load) with (a),(b) normal, (c),(d) inner race faulty, and (e),(f) outer race faulty bearing.

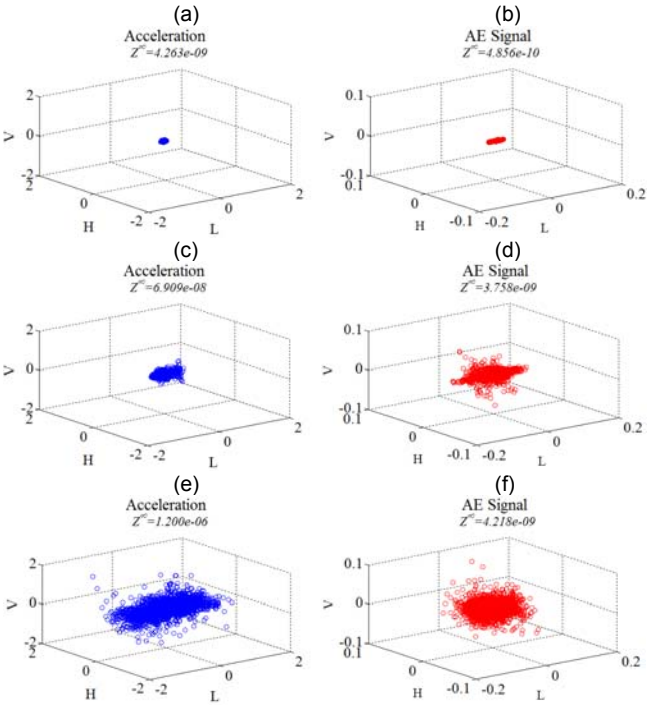

Fig. 8. Comparison of I-kaz graphic and coefficient for acceleration and AE signal of the motor running at 1380 rpm (full load) with (a),(b) normal, (c),(d) inner race faulty, and (e),(f) outer race faulty bearing.

3.3 Comparative Analysis

Comparative analysis between I-kaz and kurtosis from all recorded data (32 files) have been performed. Scatter plots for vibration and AE signal with values grouped by bearing conditions, i.e. normal, inner race faulty, and outer race faulty bearing have been compared visually. Fig. 9 and Fig. 10 shown scatter plot for the without load and with full load respectively.

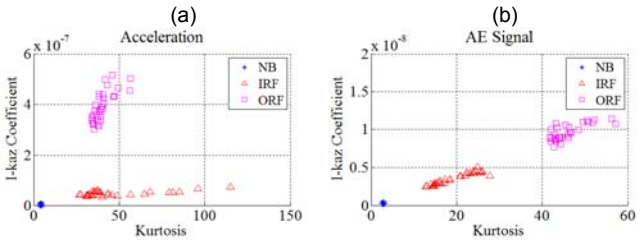

Fig. 9. Scatter plot of I-kaz coefficient vs Kurtosis for the motor running at 1450 rpm (no load).

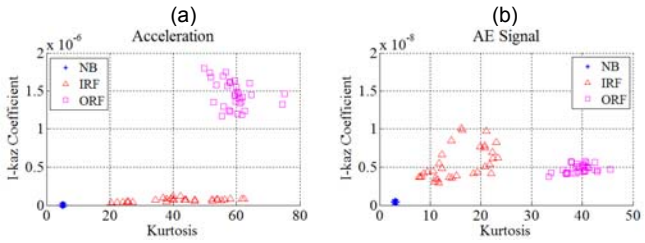

Fig. 10. Scatter plots of I-kaz coefficient vs Kurtosis for the 4 pole motor running at 1380 rpm (full load).

In all figures, normal bearing plots show consistent position compared to inner race and outer race faults with the vibration signal provided better stability compared to AE signal. Plots of acceleration and AE signal for inner race and outer race faulty bearing are scattered at different slots.

4. Conclusion

From overall experimentation results, vibration and AE signals analysis using kurtosis based methods have provided good identification to distinguish between normal and damaged bearings. On the other hand, the graphical I-kaz plot also can be quick and easy technique to detect bearing faults. Furthermore, the comparison of I-kaz coefficient against kurtosis values from all data files using the scatter plot given better clarification.

***Authors**: Ir., Mohd Sufian Othman, Dept. of Mechanical and Material Engineering, Universiti Kebangsaan Malaysia, 43600 Bangi, Selangor, Malaysia. Email: sufian@jkr.gov.my;*
Dr., associate prof, Mohd Zaki Nuawi, Dept. of Mechanical and Material Engineering, Universiti Kebangsaan Malaysia, 43600 Bangi, Selangor, Malaysia. Email: mzn@ukm.edu.my;
Dr., Ramizi Mohamed, Dept of Electrical, Electronic and System Engineering, Universiti Kebangsaan Malaysia, 43600 Bangi, Selangor, Malaysia. EmaII: ramizi@eng.ukm.my.

REFERENCES

[1] R. Bogue, “Sensors for condition monitoring: a review of technologies and applications,” *Sens. Rev.*, vol. 33, no. 4, pp. 295–299, 2013.
[2] Y. He, X. Zhang, and M. I. Friswell, “Defect Diagnosis for Rolling Element Bearings Using Acoustic Emission,” *Journal of Vibration and Acoustics*, vol. 131, no. 6. p. 061012, 2009.
[3] S. Al-Dossary, R. Hamzah, and D. Mba, “Observations of changes in acoustic emission waveform for varying seeded defect sizes in a rolling element bearing,” *Appl. Acoust.*, vol. 70, no. 1, pp. 58–81, 2009.
[4] A. M. Al-Ghamd and D. Mba, “A comparative experimental study on the use of acoustic emission and vibration analysis for bearing defect identification and estimation of defect size,” *Mech. Syst. Signal Process.*, vol. 20, no. 7, pp. 1537–1571, 2006.

[5] B. Eftekharnejad, M. R. Carrasco, B. Charnley, and D. Mba, “The application of spectral kurtosis on Acoustic Emission and vibrations from a defective bearing,” *Mech. Syst. Signal Process.*, vol. 25, no. 1, pp. 266–284, 2011.
[6] X. Liu, X. Wu, and C. Liu, “A comparison of acoustic emission and vibration on bearing fault detection,” in *2011 International Conference on Transportation, Mechanical, and Electrical Engineering (TMEE)*, 2011, pp. 922–926.
[7] N. Tandon and A. Choudhury, “A review of vibration and acoustic measurement methods for the detection of defects in rolling element bearings,” *Tribol. Int.*, vol. 32, no. 1999, pp. 469–480, 2000.
[8] D. Dyer and R. Stewart, “Detection of Rolling Element Bearing Damage by Statistical Vibration Analysis,” *J. Mech. Des.*, vol. 100, no. 2, pp. 229–235, 1978.
[9] W. Guo, P. W. Tse, and A. Djordjevich, “Faulty bearing signal recovery from large noise using a hybrid method based on spectral kurtosis and ensemble empirical mode decomposition,” *Meas. J. Int. Meas. Confed.*, vol. 45, no. 5, pp. 1308–1322, 2012.
[10] V. C. M. N. Leite, J. Guedes, G. Francimeire, C. Veloso, L. Eduardo, S. Member, G. Lambert-torres, E. L. Bonaldi, L. Ely, and D. L. De Oliveira, “Detection of Localized Bearing Faults in Induction Machines by Spectral Kurtosis and Envelope Analysis of Stator Current,” *IEEE Trans. Ind. Electron.*, vol. 62, no. 3, pp. 1855–1865, 2015.
[11] X. Zhang, J. Kang, L. Xiao, J. Zhao, and H. Teng, “A New Improved Kurtogram and Its Application to Bearing Fault Diagnosis,” *Shock Vib.*, vol. 2015, p. 22 pages, 2015.
[12] Y. Lei, J. Lin, Z. He, and Y. Zi, “Application of an improved kurtogram method for fault diagnosis of rolling element bearings,” *Mech. Syst. Signal Process.*, vol. 25, no. 5, pp. 1738–1749, Jul. 2011.
[13] M. Z. Nuawi, M. J. M. Nor, N. Jamaludin, S. Abdullah, F. Lamin, and C. K. E. Nizwan, “Development of integrated Kurtosis-based Algorithm for Z-filter technique,” *J. Appl. Sci.*, vol. 8, no. 8, pp. 1541–1547, 2008.
[14] N. I. I. Mansor, M. J. Ghazali, M. Z. Nuawi, and S. E. M. Kamal, “Monitoring bearing condition using airborne sound,” *Int. J. Mech. Mater. Eng.*, vol. 4, no. 2, pp. 152–155, 2009.
[15] M. Z. Nuawi, S. Abdullah, A. R. Ismail, R. Zulkifli, M. K. Zakaria, and M. F. H. Hussin, “A Study on Ultrasonic Signals Processing Generated From Automobile Engine Block Using Statistical Analysis,” *WSEAS Trans. Signal Process.*, vol. 4, no. 5, pp. 279–288, 2008.
[16] S. Abdullah, M. Z. Nuawi, M. Z. Nopiah, and A. Ariffin, “Study on correlation between strain and vibration signal using hybrid I-Kaz method,” *Contin. Mech. Fluids, Heat*, vol. 6, no. 3, pp. 79–88, 2010.
[17] M. Z. Nuawi, F. Lamin, A. R. Ismail, S. Abdullah, and Z. Wahid, “A Novel Machining Signal Filtering Technique: Z-notch Filter,” *World Acad. Sci. Eng. Technol. 54*, vol. 3, no. 6, pp. 24–29, 2009.
[18] M. A. F. Ahmad, M. Z. Nuawi, S. Abdullah, Z. Wahid, Z. Karim, and M. Dirhamsyah, “Development of Tool Wear Machining Monitoring Using Novel Statistical Analysis Method, I-kaz^{TM},” *Procedia Eng.*, vol. 101, pp. 355–362, 2015.
[19] J. A. Ghani, M. Rizal, A. Sayuti, M. Z. Nuawi, M. N. Ab. Rahman, and C. H. Che Haron, “New Regression Model and I-Kaz Method for Online Cutting Tool Wear Monitoring,” *World Acad. Sci. Eng. Technol. 60*, no. 2008, pp. 420–425, 2009.
[20] M. B. Ali, S. Abdullah, M. Z. Nuawi, M. M. Padzi, and K. A. Zakaria, “Experimental Analysis of an Instrumented Charpy Impact Using Statistical Study Based Data Analysis,” *Int. J. Mech. Mater. Eng.*, vol. 6, no. 2, pp. 260–268, 2011.